JJMIE

Volume 19, Number 1, March. 2025
ISSN 1995-6665
Pages 171 – 177
https://doi.org/10.59038/jjmie/190113
Editor-in-Chief: Prof. Ali M. Jawarneh

Jordan Journal of Mechanical and Industrial Engineering

# Improvement of Corrosion and Wear Resistance of (Ti12Mo5Ta) Alloy by Germanium Addition Used in Biomedical Applications

Malik Abdul-husien[1,2,a*], Haydar H.J Jamal Al Deen[1,b], Ahmed O. Al-Roubaiy [1,c]

[1] *Metallurgical Engineering, Materials Engineering College, University of Babylon, Iraq.*
[2] *Technical Institute of Babylon,Al-Furat Al-Awsat Technical University(ATU),Iraq.*

*Received 29 Sep 2024* *Accepted 25 Nov 2024*

**Abstract**

The primary objective of this investigation is to examine the impact of adding (Ge) to the Ti12Mo5Ta alloy on its corrosion resistance and wear rate. A Ti-Mo-Ta alloy with an 83% Ti, 12% Mo, and 5% Ta composition was synthesized by powder metallurgy, with the inclusion of Ge. The mixing procedure lasted for a duration of 5 hours, with a compacting pressure of 800MPa applied to create a disk sample. After the compaction step, the samples were sintered by gradually increasing the temperature to 950 ºC at a rate of 10 ˚C/min, which took a total of 7 hours. The addition of (Ge) is done in different weight percentages, ranging from 0.5% to 5%.The impact of (Ge) was examined using X-ray diffraction and SEM.the exposure of the majority of implants within the human body to corrosive environments, The addition of 0.5% to 5% (Ge) enhancement the corrosion resistance `of the Ti12Mo5Ta alloy, achieving a maximum improvement of 98.8% at 5 wt% Ge, corresponding to a corrosion rate of 2.31E-10 mpywhenreducing the porosity up to 18.7%.These prosthetic implants are subject to friction and can wear out, the addition of 0.5% to 5% (Ge) causes a decrease in the wear rate of the Ti12Mo5Ta alloy, achieving a maximum improvement of wear resistance was 99.74% at 5 wt% Ge , where the wear rate was 1.06E-08($cm^3$/N.M)by increasing the hardness up to 290 ($Kg/mm^2$).



**Keywords:** Biomaterials,corrosion resistance, wear rate, Orthopedics.

## 1. Introduction

Medical specialization is continuously advancing on a daily basis. This is the rapid advancement of orthopedics, which is accompanied by the simultaneous progress in biomaterials. The term "biomaterial" was officially defined in 1982 at the Conference of the National Institute for the Development of Consensus in Health. It refers to any substance, whether synthetic or natural, that can be used temporarily or permanently as a component of a system that treats, enhances, or substitutes any tissue, organ, or bodily function, excluding non-drugs [1]. The desire to minimize surgical interventions for the management of damaged implants has created a strong motivation for the advancement of biomaterials [2]. The national market for orthopedic implants has been steadily growing, with an estimated annual value of US $64 million. In 1999, the global value amounted to $4.4 billion. In Brazil, the annual average number of complete hip prosthetic implants performed is estimated to be 24,000[3].Anodization is a chemical process that builds and stabilizes the oxide layer on some metals and alloys [4]–[7].Interference coloring is the color of electrochemically oxidized titanium, and it is determined by the thickness of the oxide layer produced and the difference in potential applied[8]–[11].The color's created are vibrant and different, and the oxide's thickness ranges from a few nanometers to a few micrometers. Carbon, nickel, lead, titanium, platinum, or stainless steel as a conductor to the electrochemical solution at the cathode (negative pole) [12]. Extensive research and clinical evidence have shown that (CP Ti) and most Ti alloys has exceptional biocompatibility. Although their strong corrosion resistance is a role, the major mechanism of the biocompatibility of Ti (CP Ti and Ti alloys) is as yet unknown. Biological methodologies, including the observation of the interface between titanium (Ti) and adjacent tissue, the analysis of gene expression in cells on Ti, the examination for protein absorbing to Ti, the identification of the sequence of peptides of adsorbed proteins to Ti, the examination of bone formation on Ti, the study of soft tissue adhesion to Ti, and the exploration of bacteria's attachment to Ti, have been utilized to elucidate the principles of biological compatibility [13]. Connective tissue reintegration remains a primary challenge in implant-prosthetic treatment. Recent focus has been on the barrier between the surface of the trans-mucosal component and the surrounding soft tissue. Stabilizing the connection between the connective tissue and the epithelial attachment on the abutment surface (for bone-level implants) or on the implant neck (for tissue-level implants) is now considered critical for preventing bacterial infection and reducing the risk of peri-implantitis.

* Corresponding author e-mail: malik650ang@gmail.com.

Over the past decade, research has increasingly focused on improving osteointegration and enhancing implant survival rates. [14].In the past few years, metals have been considered to be extremely promising materials in medical restoration and tissue engineering. The exceptional mechanical strength of metallic biomaterials allows them to effectively maintain and replace injured tissue. Consequently, metals have been widely employed in load-bearing applications in dentistry and orthopedics. Cobalt, iron, and titanium (Ti)-based alloys are bimetals frequently utilized in vascular stents, hip joints, dentistry equipment, and orthopedics implants. Nonetheless, the alloying elements of Co- and Fe-based alloys, specifically Co, Ni, and Cr, become highly toxic when ionized within the body, hence limiting their practical use in clinical environments[15].Considerable progress in biomedical engineering has been achieved at the convergence of materials science and biomedical engineering. Leveraging this confluence, titanium, an elemental metal, has demonstrated its transformative potential as a biomaterial when appropriately alloyed. Characterized by its exceptional combination of mechanical robustness, compatibility with living organisms, resistance to corrosion, and capacity to provide integrated interactions between tissues. Specifically in the domains of orthopedics and dentistry, titanium alloys have proven to be the most effective material in biomedical applications[16]. Scientists have successfully created several biomaterials and technology for replacing joints in the human body, including metallic materials such as stainless steel, Co-Cr alloys, and Ti and its alloys. The selection of these materials is primarily based on their bulk mechanical properties, which closely resemble those of human bones, as well as their inertness towards biological tissues or fluids [17]. (Cp-Ti), which has an α-phase type structure, was mostly utilized in orthopedic and dental applications without causing any toxicity when employed in the human body [18,19,20]. However, the mechanical properties of commercial pure titanium are insufficient for specific applications that demand both resistance to wear and high strength [21, 22]. Therefore, in order to address this issue, Ti-alloys have been engineered to enhance their strength [23]. In order to fulfill the specifications of biomaterials used in biomedical applications, (Cp-Ti) was substituted by the first iteration of Ti alloys, known as Ti-6Al-4V, which consist of β+α phases [24]. While several studies have examined the desirable characteristics of Cp-Ti and first generation titanium alloy Ti-6Al-4V, there are still certain challenges that need to be addressed. New research indicates that the Cp-Ti (α-phase) and Ti-6Al-4V (α+β phase) alloys have an elastic modulus of 100 GPa, which surpasses the bone's modulus of elasticity of 20 GPa. This discrepancy results in a stress shielding effect. This stress results in bone and implant loss [9, 25,26]. In order to address these problems, numerous studies have concentrated on developing various titanium-based alloys that possess a low Young's modulus, non-allergenic and non-toxic components, and a single phase [27,28]. Experimental investigation of the impact of Mo on the microstructure and mechanical characteristics of micro-alloyed Ti with Mo. The detected microstructures comprised two forms precipitates: the martensitic an orthorhombic α" phase and the (ω) phase. Despite the incorporation of such phases in the alloys leading to increased tensile strengths, all examined alloys demonstrated elastic moduli significantly above that of human bone. Furthermore, the alloys exhibited brittle failure. Depending on the concentration of the β stabilizers, heat treatment can also regulate the phase components of an alloy[29.[The martensitic transition start temperature (Ms) can be modified by adding alloying elements. However, for biological applications, non-toxic alloying components are essential. Pure titanium transitions from its low-temperature α-phase (HCP) to the high-temperature β-phase (BCC) at 882 °C. Alloying elements such as Nb, Mo, and Ta can stabilize the high-temperature β-phase at room temperature[30]. The martensitic transformation in Ti alloys involves a transition from the β-phase (body-centered cubic, BCC) to one of two metastable phases: orthorhombic martensitic (α″) or hexagonal martensitic (α'). This transformation is highly dependent on alloy composition, with a shift from the β-phase to the α″ phase occurring at specific alloy concentrations. To accommodate the strain induced by this β-to-α″ transformation, internal twinning is commonly observed[30].Nevertheless, there exist many compositions of β titanium alloys, each with distinct microstructures including β, β+α, β+α′, β+α″, and β+ω [31].

## 2. EXPERIMENTAL WORK

The Ti 12Mo 5Ta –xGe alloys were utilized to create the specimens by the powder metallurgy process. The mean particle size and level of purity of the samples are provided in Table (1). The weighted powders were meticulously mixed using a rotating automatic ball mill, employing steel balls of different sizes. Ethanol was introduced as a wet mixing medium. The procedure of mixing was conducted for a duration of 5 hours. Fine particles powder combination, weighing 3.5 grams, was compressed using an electric hydraulic press to create a disk-shaped sample of 12 mm in diameter and 6 mm in thickness. The pressure applied during compaction was 800 (MPa), and the sample was held under this pressure for a duration of 4 minutes. The sintering process was conducted in an electrical argon furnace under Argon conditions. After the compaction stage, the samples were sintered by increasing their temperature to 950 ºC at a heat rate of 10 ˚C/min. The specimens are thereafter immersed for a duration of 7 hours and then cooled within the furnace until they achieved ambient temperature.

**Table 1.** Materials powder used in this work, together with their average particle size and purity.

| Powder | Ti | Mo | Ta | Ge |
|---|---|---|---|---|
| Average particle size(μm) | 26.43 | 29.89 | 6.433 | 4.325 |
| Purity % | 99.85 | 99.90 | 99.95 | 99.97 |

### *2.1. MICROSTRUCTURES CHARACTERIZATION*

- **X-Ray Diffraction** The Ti alloy underwent X-ray diffraction examination after sintering, and the obtained data were compared with standard charts. The test was conducted with a speed of 6 degrees per minute, a step size of 0.02 degrees, and an angle range of 20-80

degrees with a copper (Cu) target. The wavelength employed was 1.54060 Angstroms, the voltage was 40 kilovolts, and the current was 30 mill amperes.

- **Microstructure Observation** After the sintering process, all samples were subjected to grinding using silicon carbide sheets with varying grit sizes, namely 180, 400, 600, 800, 1000, 1200, 1500, and 2000. Afterwards, the samples were polished using diamond paste in order to attain a glossy and reflective finish, which served as the final phase. The etching procedure was performed at room temperature. Table 2 displays the chemical composition of the etching solution[32]. Subsequent to the etching process, the samples had been rinsed with water and dried. They were then inspected under 400x magnification using optical microscopy and scanning electron microscopy. Characteristics such as the identification of phases, shape, and grain size are included in the analysis of grain boundaries. Each of these possesses unique attributes.

**Table 2.** Etching solution composition [32].

| NO | Constituents | ml |
|---|---|---|
| 1 | HF | 10 ml |
| 2 | $HNO_3$ | 5 ml |
| 3 | $H_2O$ | 85 ml |

### *2.2. CORROSION TEST*

Polarization experiments were conducted utilizing an electrochemical standard cell comprising a working electrode, an auxiliary electrode (platinum), and a reference electrode (saturated calomel electrode) in Ringer solution, in accordance with the American Society for Testing and Materials (ASTM) standards [33].Polarisation tests have been performed using a potentiostat of the Winking M Labf200 model. Upon reaching a constant potential, potentiodynamic polarisation commences from a first potential of 250 mV under the open circuit potential and continues to 800 mV over the open circuit potential. The specimens were scanned in the positive direction at a rate of sweep of 0.4 mV/s, and the current was recorded in relation to the potential. The corrosion potentials (Ecorr) and corrosion current density (Icorr) are determined from the test, and the corrosion rate is calculated using the following equation (1) [33].

$$\text{Corrosion Rate(mpy)} = [(0.13 i_{cor}.(E.W))/\rho] \quad (1)$$

Where:
E.W: equivalent weight (g/eq.)
ρ: density (g/cm$^3$)
Icorr: current density (μA/cm$^3$)

### *2.3. WEAR TEST*

The dry sliding wear are studied by using pin on disk device (MT-4003, version 10). In the test using (300 rpm) and constant radius (4mm) with different sliding distance and the loads were (10N and 20N). The specimen is weighed prior to testing using an electric balance with an accuracy of 0.0001. After specified intervals (5, 10, 15, 20, 25, and 30 minutes), the specimens are weighed, and the dry sliding wear rate is calculated according to Equation (2) and The test method had been covered according to ASTM G 99[34].

$$\text{Volume Loss} = [\text{weigh loss (g)}/\rho] \quad (2)$$

Where:
Weight loss (g)= quantity loss after(5, 10, 15, 20, 25 and 30 )min.
ρ (g/cm$^3$) = final density.
Wear rate calculated from the following equation (3)[35].

$$Wa = \Delta G/d \times p \times s \quad (3)$$

Where:
Wa:is the wear rate, (cm$^3$/N.m).
ΔG: is the weight loss, (g).
D: is the density, (g/cm$^3$).
P: is the load, (N).
s: is the sliding distance, (m).

## 3. RESULT AND DISCUSSION

### *3.1. MICROSTRUCTURE CHARACTERIZATION*

The (XRD) patterns of the green compact alloys exhibit only the presence of titanium (Ti), molybdenum (Mo), tantalum (Ta), and germanium (Ge) phases. This is because there is no occurrence of phase change during the compacting process. Phase transformation is a type of diffusion process that requires a high temperature in order to take place. Figure (1) displays the (XRD) patterns of the base alloy (Ti12Mo5Ta) after undergoing sintering at a heat of 950 °C for a duration of 7 hours in an argon atmosphere. It is evident that Ti, Mo, and Ta underwent transformation into two solid solutions, namely αTi and βTi.

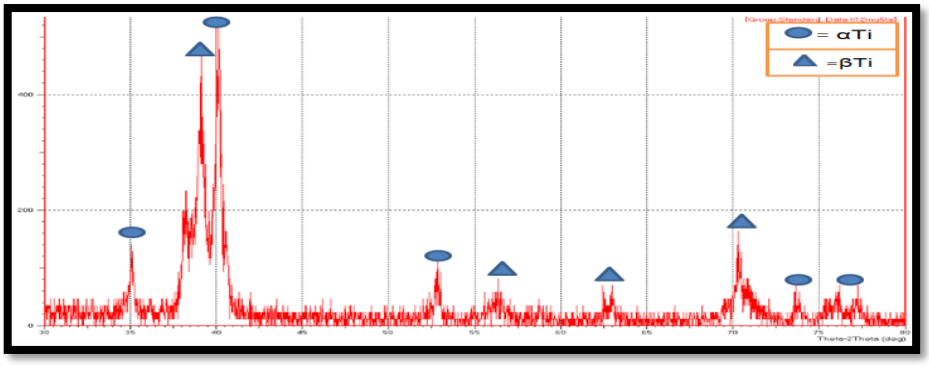


**Figure 1.** XRD patterns of (Ti12Mo5Ta) after sintering process.

Figure (2) depicts (XRD) pattern of the base alloy (Ti12Mo5Ta) with 5% Ge after undergoing the sintering process at a heat of 950°C for a duration of 7 hours in an Argon gas atmosphere. The graphic displays the transformation of the basic elemental substances Ti, Mo, Ta, and Ge into αTi, βTi, and $Ti_6Ge_5$. However, the figure does not show any peaks corresponding to metallic Ti, Mo, Ta, and Ge. The sintering process length of 7 hours was sufficient to fully complete the phase transformation process, as it enhanced the interdiffusion between (Ti), (Mo), (Ta), and (Ge). The presence of free elements in alloys used as biomaterials is avoided due to their harmful effects on the organism.

Figures (3a)-(5a) display the microstructure of etched alloys following the sintering process, both with and without the addition of Ge, at a magnification of 400X. The borders of the grains and the existing phases were identified by examining the microstructure of these alloys. The specimens, after undergoing the sintering process, were found to possess a microstructure consisting of two distinct regions, known as a duplex microstructure. One part appears light (bright) and consists of the α-Ti phase, while the other sections appear dark, indicating the presence of the (β-phase). The presence of Mo and Ta elements results in the promotion of the dark reign (β-phase) due to their role as stabilizing factors for the β phase. By increasing the quantity of germanium, the shaded region is raised. At room temperature, there are some beta phases in equilibrium, which is analogous to α-β and β alloys [36].SEM images of the etched alloys, shown in Figures 3b–5b, display the α-Ti and β-Ti phases, grain boundaries, and pores of varying sizes. Due to the metal powder method used in specimen preparation, the SEM examination reveals a limited number of surface pores, which decrease as the germanium content increases. This reduction in porosity, attributed to germanium's role in modifying the alloy structure, enhances the corrosion resistance of the material.The use of the powder metallurgy process in alloys results in a uniform distribution of the strengthening phase throughout the matrix, Consequently, enhancing the alloys ability to withstand wear and boosting their mechanical characteristics. The microstructure demonstrates the existence of intermetallic phase ($Ti_6Ge_5$) as depicted in XRD figure (2), resulting in enhanced hardness of the alloy and improved mechanical properties with higher germanium content.

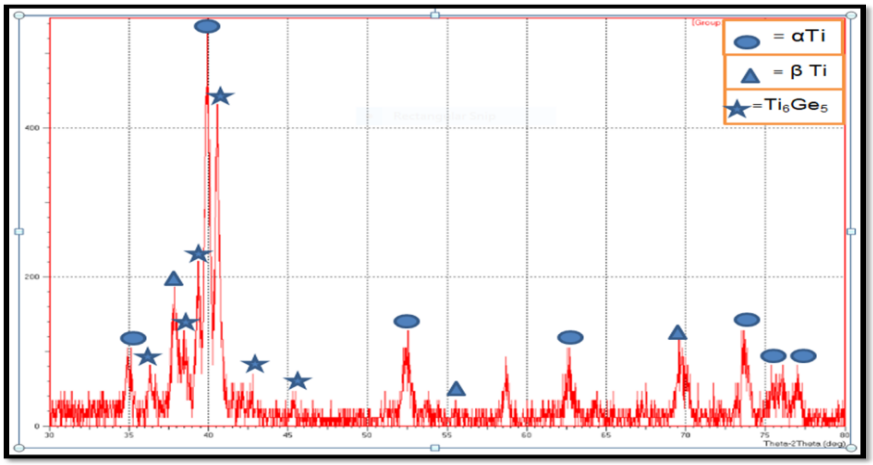


**Figure 2**. XRD patterns of (Ti12Mo5Ta) with 5% Ge after the sintering process.

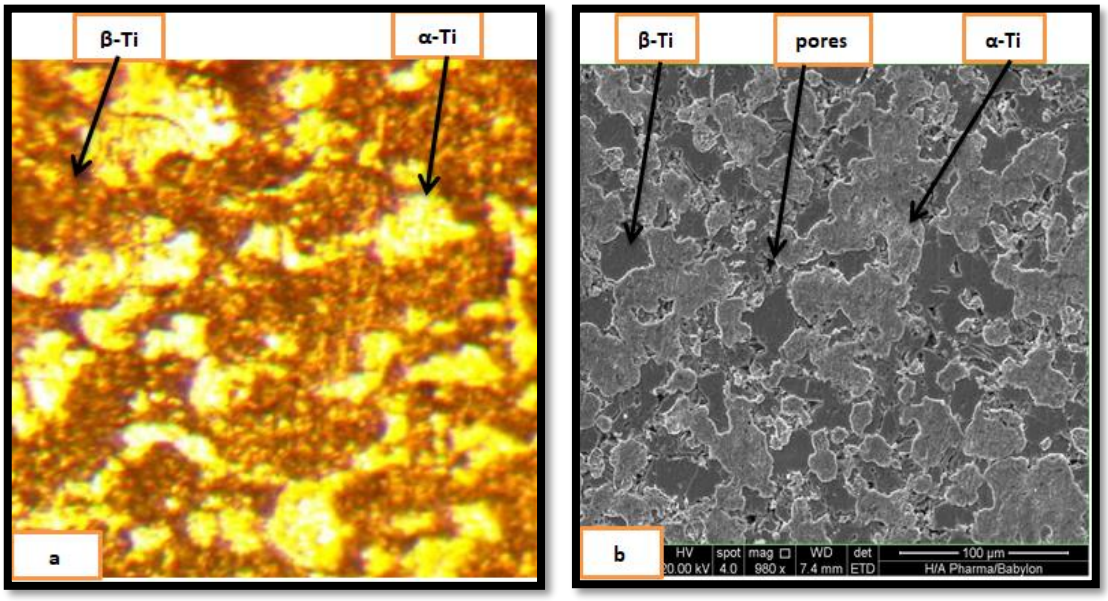


**Figure 3.** The microstructure observation of (base). a) Utilizing the Optical Microscope at a resolution of 400X. b) Through the (SEM).

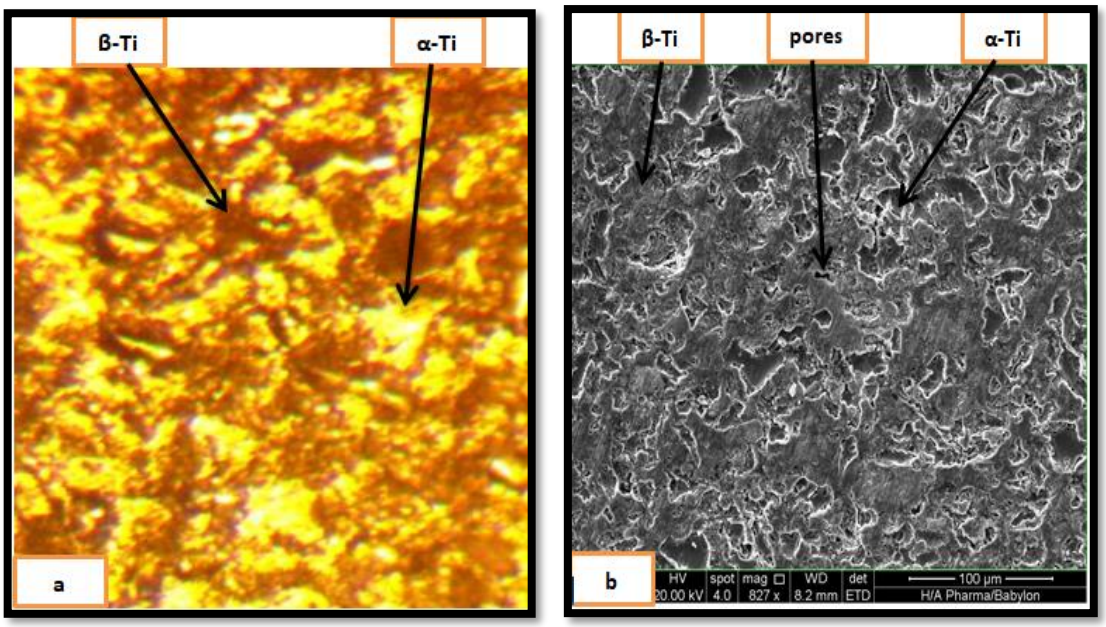


**Figure 4.** The microstructure observation of (2.5 % Ge addition). a) Utilizing the Optical Microscope at a resolution of 400X. b) Through the (SEM).

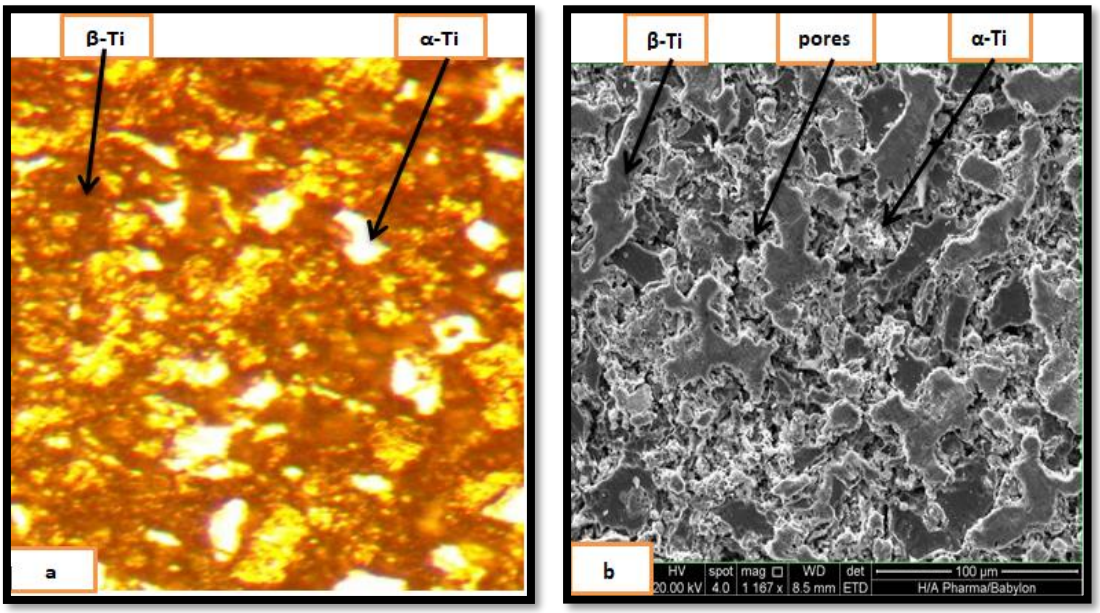


**Figure 5.** The microstructure observation of (5 % Ge addition). a) Utilizing the Optical Microscope at a resolution of 400X. b) Through the (SEM).

### *3.2. CORROSION TEST*

The electrochemical corrosion utilizing one sample of each (Ti12Mo5Ta and Ti12Mo5Ta-xGe). The schematic current-potential curves, known as polarization curves, are depicted in Figure 6, illustrating the cathodic and anodic polarization characteristics of Ti12Mo5Ta and Ti12Mo5Ta-xGe in Ringer solution at 37±1 ºC.Figure (6) illustrates the polarization curves for the base alloy and the base alloy with Ge addition. During cathodic polarization, the voltage escalates while the current diminishes until it attains the minimum attainable value. During anodic polarization, the voltage escalates as the current intensifies. The simultaneous increase in voltage and current indicates active anodic polarization behavior, demonstrating the ongoing dissolution of metal. The shape of the anodic curve evidences the presence of a passive region in both the base alloy and the base alloy with Ge addition. The corrosion current densities, corrosion potentials, and the computed corrosion rate data from these curves are illustrated in Figure 6.

Table (3) demonstrates a notable enhancement in the corrosion resistance of the base alloy with varying concentrations of Gebecause decrease of porosity : 0.5% (0.5%), 1% (72.4%), 1.5% (77.2%), 2% (80.6%), 2.5% (81.4%), 3% (83.3%), 3.5% (87.1%), 4% (90.6%), 4.5% (97.9%), and 5% (98.8%).The Icorr density for the specimens ranges from 3.17E-10 (µA/cm²) for 0.5% (Ge) to 2.41E-12 (µA/cm²) for 5% (Ge), both of which are lower than the Icorr of the base alloy, measured at 1.68E-10 (µA/cm²). The Ecorr values range from -225 mV for

 

0.5% (Ge) to -13 mV for 5% (Ge), both of which exceed the Ecorr of the base alloy, which is -300 mV.Porosity is reduced and corrosion resistance is raised with the addition of Ge.. Titanium alloys can be made into a protective layer on the surface that reduces into the rate of corrosion.

### *3.3. WEAR TEST*

The inclusion of Ge enhances wear resistance, as seen by the correlation between increased Ge percentage and improved wear resistance. This phenomenon can be attributed to the formation of the intermetallic complex ($Ti_6Ge_5$), which contributes to the increased hardness of all germanium-containing alloys. Table (4) shows the Brinell hardness(HB)and improvement percentage in wear resistance of the base alloy (Ti12Mo5Ta) with respect to the addition of Ge. We notice from the above figures that when loads (10N and 20N) are applied, the wear rate at (20N) is greater than that of (10N) because of increasing friction coefficient when the wear rate for base alloy is (2.30 * 10^-6, 4.22 * 10-6) ($cm^3$/N.M) at (10N & 20N) respectively. The wear rate initially increases at 10N and 20N until it reaches its peak value. However, with an increase in germanium content, the wear rate stabilizes and reaches a steady state. The reason for the initial increase in wear rate is the reduced resistance on the surface, allowing for easier removal of convexity and concavity layers. This process continues until the wear rate stabilizes, indicating the attainment of a steady friction coefficient.

The effect of Ge content on wear rate of base alloy and base alloy with Ge addition under constant load (20N) and constant time (30min), it can be noted that the wear rate decreases with increasing Ge content, the wear rate of 0.5% Germanium alloy is (2.13*10-6 $cm^3$/N.M) compared to that of base alloy (4.22*10-6 $cm^3$/N.M) which achieved improvement percentage of (49.52%).The wear resistance improvement increases with increasing Germanium content until reach (99.74%) at 5% Germanium, This improvement can be attributed to the strengthening effect of intermetallic compounds. The wear rate is reduced by the inclusion of Germanium, which minimizes porosity and increases the hardness of the alloyThis can be attributed to the strengthening effect of the intermetallic compound ($Ti_6Ge_5$). The effect of Germanium content on wear rate shown in figure (7).

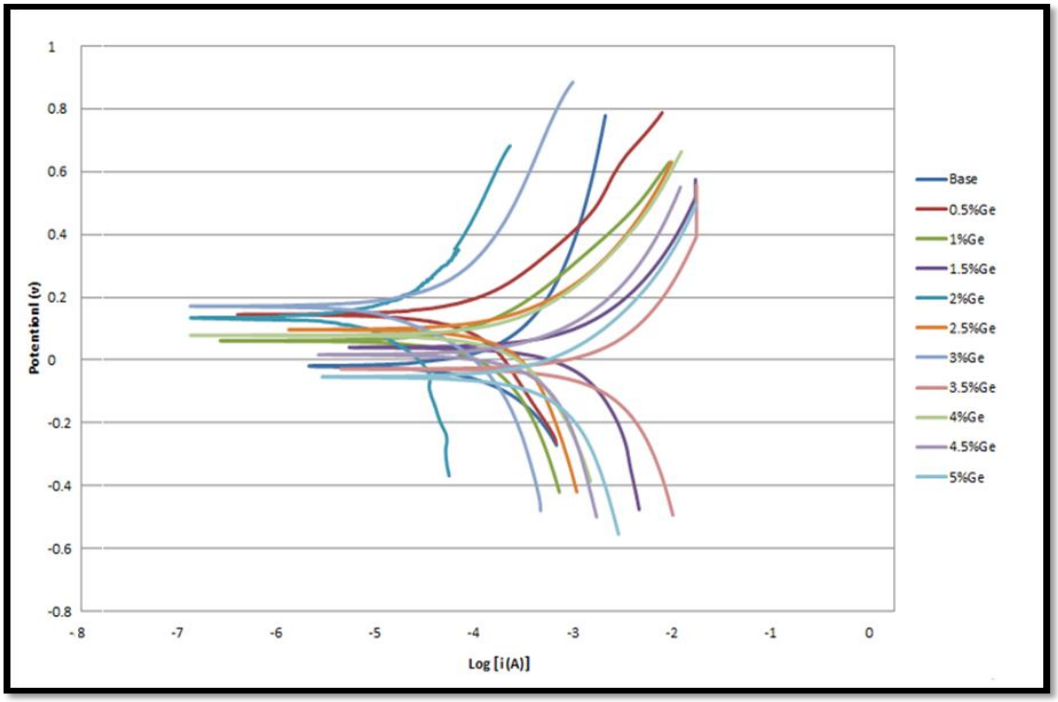


**Figure 6.** The Leaner polarization curves of each (base alloy and base alloy with Ge addition).

**Table 3.** Illustrates the porosity, corrosion potential (Ecorr), corrosion current density (Icorr), corrosion rate and improvement **percentage.**

| Ge(%) | Porosity(%) | Icorr. (μA/$cm^2$) | Ecorr.(mv) | corrosion rate (C.R)mpy | Improvement percentage(%) |
|---|---|---|---|---|---|
| 0 | 33.4 | 1.68E-10 | -300 | 1.99E-08 | |
| 0.5%Ge | 32.7 | 3.17E-10 | -225 | 1.98E-08 | 0.502 |
| 1%Ge | 30.4 | 1.91E-11 | -181 | 5.49E-09 | 72.412 |
| 1.5%Ge | 28.2 | 9.53E-11 | -170 | 4.53E-09 | 77.236 |
| 2%Ge | 26.4 | 7.41E-11 | -165 | 3.86E-09 | 80.603 |
| 2.5%Ge | 25.6 | 4.54E-11 | -150 | 3.69E-09 | 81.457 |
| 3%Ge | 23.9 | 2.04E-11 | -148 | 3.31E-09 | 83.366 |
| 3.5%Ge | 22.2 | 4.49E-11 | -118 | 2.55E-09 | 87.185 |
| 4%Ge | 21.6 | 2.57E-11 | -85 | 1.86E-09 | 90.653 |
| 4.5%Ge | 20.1 | 5.79E-12 | -37 | 4.12E-10 | 97.929 |
| 5%Ge | 18.7 | 2.41E-12 | -13 | 2.31E-10 | 98.839 |

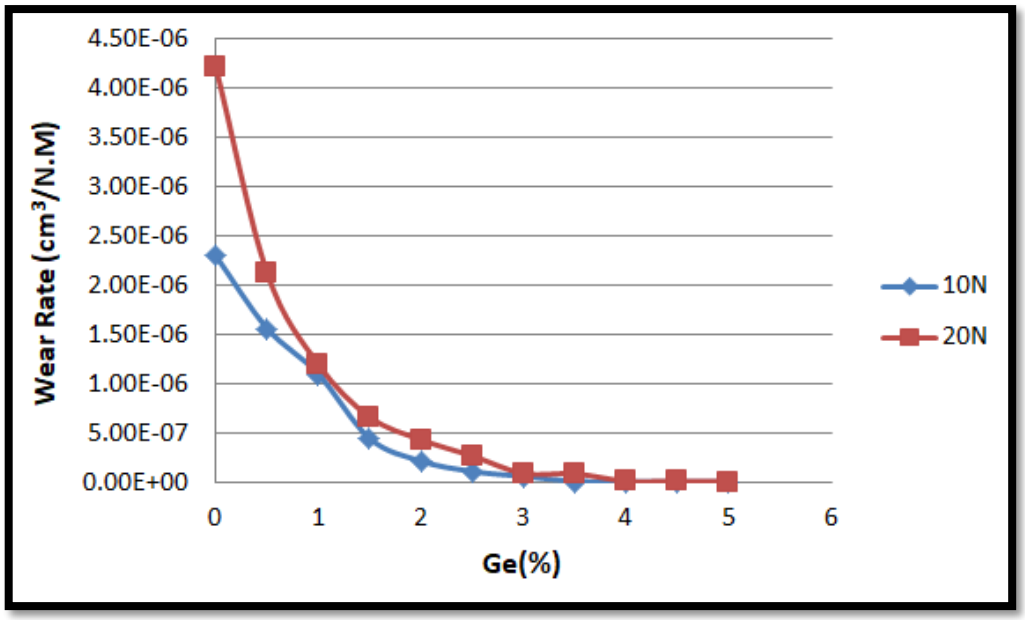


**Figure 7.** The effect of Germanium content on wear rate.

**Table 4.** Hardness, Wear Rate and Improvement Percentage% at (10N & 20N).

| Ge(%) | HB (Kg/mm$^2$) | Wear Rate(cm$^3$/N.M) at 30min | | Improvement (%) at 20N |
|---|---|---|---|---|
| | | 10N | 20N | |
| 0 | 185 | 2.30E-06 | 4.22E-06 | |
| 0.5%Ge | 194 | 1.56E-06 | 2.13E-06 | 49.52 |
| 1%Ge | 212 | 1.10E-06 | 1.20E-06 | 71.56 |
| 1.5%Ge | 220 | 4.47E-07 | 6.63E-07 | 84.28 |
| 2%Ge | 234 | 2.17E-07 | 4.33E-07 | 89.73 |
| 2.5%Ge | 246 | 1.11E-07 | 2.69E-07 | 93.62 |
| 3%Ge | 256 | 6.11E-08 | 9.04E-08 | 97.85 |
| 3.5%Ge | 268 | 1.12E-08 | 8.84E-08 | 97.9 |
| 4%Ge | 274 | 6.12E-09 | 1.22E-08 | 99.71 |
| 4.5%Ge | 281 | 5.81E-09 | 1.16E-08 | 99.72 |
| 5%Ge | 290 | 5.44E-09 | 1.06E-08 | 99.74 |

## 4. CONCLUSION

1. The use of germanium enhanced the corrosion resistance of the (Ti12Mo5Ta) alloys. The corrosion resistance enhances with elevated Ge concentration, achieving a maximum improvement of 98.8% at 5 wt% Ge, corresponding to a corrosion rate of 2.31E-10 mpy.
2. The inclusion of Germanium enhanced the wear resistance of the (Ti12Mo5Ta) alloy, with wear resistance increasing proportionally to the Ge content. the maximum improvement of wear resistance was 99.74% at 5 wt% Ge , where the wear rate was 1.06E-08(cm$^3$/N.M).
3. The inclusion of Germanium to (Ti12Mo5Ta) alloy results in the formation of the ($Ti_6Ge_5$) phase, which leads to increasing the hardness up to 290 Kg/mm$^2$ at 5%Ge.
4. The inclusion of Germanium to (Ti12Mo5Ta) alloy leads to reducing the porosity up to 18.7% at 5%Ge, which leads to reducing the corrosion rate .

## REFERENCES

[1] Al-Humairi, Amir N. Saud, et al. BIOMATERIALS: Multidisciplinary approaches and their related applications. White Falcon Publishing, 2020.

[2] Vallet-Regí, María. "Evolution of bioceramics within the field of biomaterials." Comptes Rendus. Chimie 13.1-2 (2010): 174-185.

[3] Kunčická, Lenka, Radim Kocich, and Terry C. Lowe. "Advances in metals and alloys for joint replacement." Progress in Materials Science 88 (2017): 232-280.

[4] R. Das, M. K. Pradhan, and C. Das, “Prediction of surface roughness in Electrical Discharge Machining of SKD 11 TOOL steel using Recurrent Elman Networks,” Jordan Journal of Mechanical and Industrial Engineering, vol. 7, no. 1, 2013.

[5] A. Ismail, R. Zenasni, K. S. M. Amine, and S. Ahmed, “Effect of tempering temperature on the mechanical properties andmicrostructure of low alloy steel DIN 41Cr4,” Jordan Journal of Mechanical and Industrial Engineering, vol. 13, no. 1, pp. 9–14, 2019.

[6] S. Dwivedi and S. Sharma, “Optimization of Resistance Spot Welding Process Parameters on Shear Tensile Strength of SAE 1010 steel sheets Joint using Box-Behnken Design.,” Jordan Journal of Mechanical and Industrial Engineering, vol. 10, no. 2, 2016.

[7] Y. Liu, L. He, and S. Yuan, “Wear Properties of Aluminum Alloy 211z. 1 Drilling Tool.,” Jordan Journal of Mechanical and Industrial Engineering, vol. 15, no. 1, 2021.

[8] A. R. I. Kheder, N. M. Jubeh, and E. M. Tahah, “Fatigue Properties under Constant Stress/Variable Stress Amplitude and Coaxing Effect of Acicular Ductile Iron and 42 CrMo4 Steel.,” Jordan Journal of Mechanical and Industrial Engineering, vol. 5, no. 4, 2011.

[9] R. N. Hwayyin and A. S. Ameed, “The Time Dependent Poisson’s Ratio of Nonlinear Thermoviscoelastic Behavior of Glass/Polyester Composite.,” Jordan Journal of Mechanical and Industrial Engineering, vol. 16, no. 4, 2022.

[10] M. D. Al-Tahat and A.-R. Abbas, “Activity-based cost estimation model for foundry systems producing steel castings.,” Jordan Journal of Mechanical and Industrial Engineering, vol. 6, no. 1, 2012.

[11] M. Hamdan, M. Shehadeh, A. Al Aboushi, A. Hamdan, and E. Abdelhafez, “Photovoltaic Cooling Using Phase Change Material.,” Jordan Journal of Mechanical and Industrial Engineering, vol. 12, no. 3, 2018.

[12] A. H. Haleem, N. S. Radhi, N. T. Jaber, and Z. Al-Khafaji, “Preparation and Exploration of Nano-Multi-Layers on 316l Stainless Steel for Surgical Tools,” Jordan Journal of Mechanical and Industrial Engineering (JJMIE), vol. 18, no. 2, 2024.

[13] Hanawa, Takao. "Biocompatibility of titanium from the viewpoint of its surface." Science and Technology of Advanced Materials 23.1 (2022): 457-472.

[14] Hussein, Eman Yasir, Jassim M. Salman Al-Murshdy, and Nabaa Sattar Radhi. "Surface Improvement of Titanium Alloys for Biomedical Applications by Anodizing." Jordan Journal of Mechanical & Industrial Engineering 18.3 (2024).

[15] Jung, Hyun-Do. "Titanium and Its alloys for biomedical applications." Metals 11.12 (2021): 1945.

[16] Marin, Elia, and Alex Lanzutti. "Biomedical applications of titanium alloys: a comprehensive review." Materials 17.1 (2023): 114.

[17] Chakraborty, Rajib, et al. "MWCNT reinforced bone like calcium phosphate—Hydroxyapatite composite coating developed through pulsed electrodeposition with varying amount of apatite phase and crystallinity to promote superior osteoconduction, cytocompatibility and corrosion protection performance compared to bare metallic implant surface." Surface and Coatings Technology 325 (2017): 496-514.

[18] Li, Yuhua, et al. "New developments of Ti-based alloys for biomedical applications." Materials 7.3 (2014): 1709-1800.

[19] Long, Marc, and H. J. Rack. "Titanium alloys in total joint replacement—a materials science perspective." Biomaterials 19.18 (1998): 1621-1639.

[20] Hanawa, Takao. "Recent development of new alloys for biomedical use." Materials science forum. Vol. 512. Trans Tech Publications Ltd, 2006.

[21] Hussein, Mohamed A., Abdul Samad Mohammed, and Naser Al-Aqeeli. "Wear characteristics of metallic biomaterials: a review." Materials 8.5 (2015): 2749-2768.

[22] Oliveira, V., et al. "Preparation and characterization of Ti-Al-Nb alloys for orthopedic implants." Brazilian Journal of Chemical Engineering 15 (1998): 326-333.

[23] ZHU, Yuntian T., et al. Ultrafine-grained titanium for medical implants. U.S. Patent No 6,399,215, 2002.

[24] More, N. S., et al. "Tribocorrosion behavior of β titanium alloys in physiological solutions containing synovial components." Materials Science and Engineering: C 31.2 (2011): 400-408.

[25] Banerjee, Rajat, et al. "Involvement of in vivo induced cheY-4 gene of Vibrio cholerae in motility, early adherence to intestinal epithelial cells and regulation of virulence factors." FEBS letters 532.1-2 (2002): 221-226.

[26] Gross, S. T., and E. W. Abel. "A finite element analysis of hollow stemmed hip prostheses as a means of reducing stress shielding of the femur." Journal of Biomechanics 34.8 (2001): 995-1003.

[27] Geetha, Manivasagam, et al. "Ti based biomaterials, the ultimate choice for orthopaedic implants–a review." Progress in materials science 54.3 (2009): 397-425.

[28] Niinomi, Mitsuo, Masaaki Nakai, and Junko Hieda. "Development of new metallic alloys for biomedical applications." Acta biomaterialia 8.11 (2012): 3888-3903.

[29] Raganya, Mampai L., et al. "Microstructure and tensile properties of heat treated Ti-Mo alloys." (2022).

[30] Shahee, Sura Ali, and Nabaa Sattar Radhi. "Effect of Nb Content on Behavior of (Ti-Nb) Shape Memory Alloys for Biomedical Applications." Jordan Journal of Mechanical & Industrial Engineering 18.2 (2024).

[31] Ikedaa, M., M. Ueda, and M. Ninomi. "Recent studies and developments in titanium biomaterials." MATEC Web of Conferences. Vol. 321. EDP Sciences, 2020.

[32] ASTM, N. "Standard practice for microetching metals and alloys." Unided Stated of America: ASTM (2005).

[33] Gordin, D. M., et al. "WITHDRAWN: synthesis, structure and electrochemical behavior of a beta Ti–12Mo–5Ta alloy as new biomaterial." Materials letters 59.23 (2005): 2959-2964.

[34] Duerig, T., A. Pelton, and D. J. M. S. Stöckel. "An overview of nitinol medical applications." Materials Science and Engineering: A 273 (1999): 149-160.

[35] Şimşek, Ijlal, and Dursun Özyürek. "Investigation of Wear and Corrosion Behaviors of Ti15Mo Alloy Produced by Mechanical Alloying Method in SBF Environment." Powder Metallurgy and Metal Ceramics 58.7 (2019): 446-454.

[36] Huber, Daniel Edward. Structure and properties of titanium tantalum alloys for biocompatibility. Diss. The Ohio State University, 2016.